Sol–Gel Processes

Deutsche Ausgabe: DOI: 10.1002/ange.201501001
Internationale Ausgabe: DOI: 10.1002/anie.201501001

Sol Processing of Conjugated Carbon Nitride Powders for Thin-Film Fabrication**

*Jinshui Zhang, Mingwen Zhang, Lihua Lin, and Xinchen Wang**

Abstract: *The chemical protonation of graphitic carbon nitride (CN) solids with strong oxidizing acids, for example HNO_3, is demonstrated as an efficient pathway for the sol processing of a stable CN colloidal suspension, which can be translated into thin films by dip/disperse-coating techniques. The unique features of CN colloids, such as the polymeric matrix and the reversible hydrogen bonding, result in the thin-film electrodes derived from the sol solution exhibiting a high mechanical stability with improved conductivity for charge transport, and thus show a remarkably enhanced photo-electrochemical performance. The polymer system can in principle be broadly tuned by hybridization with desired functionalities, thus paving the way for the application of CN for specific tasks, as exemplified here by coupling with carbon nanotubes.*

Carbon finds diverse applications in modern society that range from catalysis, batteries, adsorption, to separation,[1] and its development has experienced an evolution from graphite and activated carbon to fullerenes, carbon nanotubes, and more recently to graphene—a single atomic sheet of graphite.[2] Substitution of carbon by nitrogen in the sp^2-bonded planar/curved π-conjugated structure can create new functionality, for example, optoelectronic activity by opening the electronic band gap of the graphite and graphene, which are zero-bandgap materials in their pristine forms.[3] This allows control over the operation of devices such as p-n junctions, transistors, and diodes.[3c] Recent studies have already shown such N-containing carbon materials/devices to have great promise for photocatalysis with visible light,[4a,b] as well as for non-Pt electrocatalysts in fuel cells.[4c–f] The solution processing of these covalent solids is crucial for further manipulation of the electronic and optoelectronic nanodevices, but it remains challenging because the covalent and interlayer cohesive energies are as high as those of graphite.[5] Herein, we show that chemistry paves the way for sol processing of a polymeric nitride semiconductor on the basis of CN with a defect graphitic structure, which has been widely adopted as an energy transducer for artificial photosynthesis.[6]

The solid-state CN was prepared by thermal-induced self-polymerization of cyanamide at 823 K, which resulted in a condensed CN solid.[6a] Although milled CN powders show photocatalytic activity, the fabrication of thin-film samples for applications in (photo)electrochemistry meet with limited success, because of the poor contact between the large aggregated particles and substrates as well as the abundant boundary defects.[7] The CN thin films are generally prepared by physical methods under non-equilibrium conditions, such as plasma jet chemical vapor deposition and pulsed-laser deposition, and the resultant films have proved difficult to characterize because of poor crystallinity and are deficient in nitrogen, which greatly restricts their photoinduction performances.[8] The development of a soft-chemistry approach for the manufacture of robust CN thin films with well-developed electronic structures is therefore desirable.[9] Although sol-gel techniques have been widely used for the fabrication of thin films and coatings of metal oxides,[10] the application of sol-gel approaches for processing nitride-related materials has been rather rare.

The most accepted CN system is an N-bridged "poly(tri-*s*-triazine)" known as Liebig's "melon" because of its high thermodynamic stability.[6] The material is stable up to about 873 K, and doesn't dissolve in most organic solvents, which makes the thin-film processing of CN virtually impossible by traditional sol-gel chemistry.[6] Theoretical calculations and experimental characterizations, however, revealed that melon units are stacked together through hydrogen bonds between the strand nitrogen atoms and NH/NH_2 groups, which in principle can act as proton-acceptor sites to form a local substructure similar to ammonium ion species (Scheme 1).[6a,11] This suggests the potential fabrication of a colloidal suspension of CN by a series of controlled protonation and depolymerization reactions under certain conditions. The

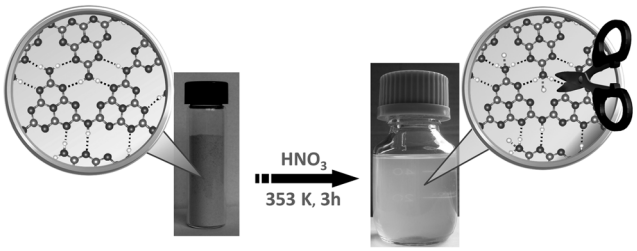

Scheme 1. Illustration of the synthesis of a CN-Sol solution. The carbon atoms are light gray, nitrogen atoms are dark gray, and hydrogen atoms are white.

[*] Dr. J. Zhang, M. Zhang, L. Lin, Prof. X. Wang
State Key Laboratory of Photocatalysis on Energy and Environment
College of Chemistry, Fuzhou University
Fuzhou 350002 (China)
E-mail: xcwang@fzu.edu.cn
Homepage: http://wanglab.fzu.edu.cn

[**] This work was financially supported by the National Basic Research Program of China (2013CB632405), the National Natural Science Foundation of China (21425309 and 21173043), the State Key Laboratory of NBC Protection for Civilian (SKLNBC2013-04K), and the Specialized Research Fund for the Doctoral Program of Higher Education (20133514110003).

Supporting information for this article is available on the WWW under http://dx.doi.org/10.1002/anie.201501001.

protonation of CN with hydrochloric acid has indeed been demonstrated previously for surface functionalization of this material, but a sol solution was not formed, presumably because of the weak acid strength and its low oxidizing ability.[12]

As a continuing effort to chemically protonate CN powder, a stronger oxidizing acid, nitric acid (HNO_3), was thus employed as the medium for the solution processing of a colloidal suspension of CN. As shown in Scheme 1, protons can easily intercalate into the layered structure of CN solids and selectively attach to the strand nitrogen atoms in a manner similar to a Brønsted acid/base interaction, thereby greatly swelling the bulk matrix and making it ready for depolymerization.[11c] In contrast to the way that HCl functionalizes the surface, NO_3^- plays a rather important role in the sol processing of CN, because of its powerful oxidizing strength. Previous reports have already demonstrated that the structural hydrogen bonding between melon units can be broken by oxidation with $KMnO_4$, thereby facilitating the depolymerization of CN solids.[11b] Thus, CN solids were heated at reflux in a concentrated HNO_3 solution (65 wt%) at 353 K to produce a stable colloidal solution, namely, CN-Sol (Scheme 1). As a consequence of the soft nature of the polymeric matrix and the reversibility of hydrogen-bond formation, the colloids contained in CN-Sol repolymerize to larger ones by re-establishing the extended π-conjugation systems after complete removal of HNO_3 by direct heating above 623 K. This is called the "gelling" process here, as it is an important step in the sol-gel engineering of thin films on various substrates. This unique colloidal behavior is rather beneficial for the fabrication of CN-based optical films without significant boundary defects, but also for proton carrier membranes with advanced applications.

Firstly, the obtained CN-Sol solution was examined with a green laser light ($\lambda = 532$ nm) to study the colloidal properties. A typical Tyndall effect is clearly evident in the CN-Sol solution, as indicated by the beam passing through the transparent sol solution (Figure 1a). This visual observation demonstrates the successful processing of a sol solution by controllable protonation with HNO_3. The particle size of the colloids contained in the CN-Sol was determined by ZetaPlus analysis (Figure 1b). The particle sizes exhibit a perfect Gaussian distribution with an average size of 310.3 nm and a standard deviation of 4.3 nm, which indicates that the CN solids are indeed depolymerized as uniform colloids. UV/Vis absorption and photoluminescence (PL) spectra were collected to determine the physicochemical properties of the CN colloids, in particular the semiconductive electronic structures, and to see if they are chemically destroyed by the HNO_3 protonation. The semiconductive electronic band structure is still present in the CN colloids (Figure 1c), but with an evident hypsochromic shift of the absorption edge from 460 to 370 nm. This increase in the bang gap is mainly caused by the protonation of the carbon nitride frameworks, which partially reduces delocalization of the π-conjugation system.[6,7,12] As a result of band gap enlargement, the corresponding PL emission band shifts towards shorter wavelength (Figure 1d). These important findings meant that we proceeded to manipulate the CN-Sol for photochemically relative applications. The blue-shifted emission of the CN colloids devalues its photochemical applications, but this effect can be counteracted in the subsequent thin-film fabrication process by a gelling process which reconnects the conjugated system on sintering at high temperatures.

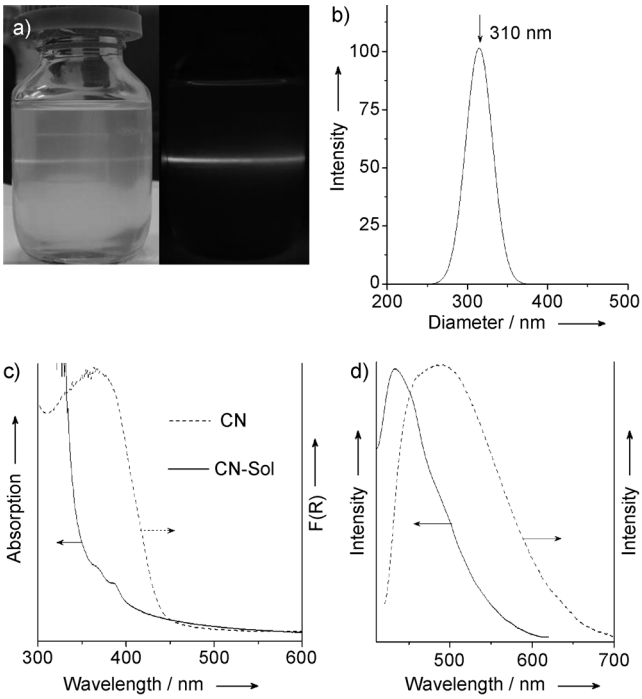

Figure 1. Physical characterization of a CN-Sol solution, together with CN solids as the reference. a) Tyndall effect generated by a green laser; b) particle-size distribution; c) UV/Vis absorption spectra; d) PL spectra under excitation at 350 nm.

The surface morphologies of the CN thin films were imaged by scanning electron microscopy (SEM). Highly interconnected porous networks without significant particle boundaries are observed in the CN-Sol thin film (TF-CN-Sol; Figure 2a). To the best of our knowledge, this typical sol-derived morphology is not only beneficial for mass transfer in film electrodes, but more importantly can greatly minimize the boundary defects to facilitate charge transport.[9] In contrast, the traditional thin film made from CN solids (TF-CN) is mainly composed of particles ranging in size from tens to thousands of nanometers, with abundant particle boundaries.[12] This kind of architecture is kinetically unfavorable experimentally. Another advantage of sol processing is that the poor contact between the CN and substrate glass can be significantly improved. Annealing the soft colloids will generate firm coating layers on the substrates with close contacts (see Figure S1 in the Supporting Information), thereby making the film rather robust against scraping with a fingernail. Electrochemical impedance spectroscopy (EIS) was carried out to examine the electronic conductivity (Figure 2c).[7a] Compared with the film before annealing (TF-CN-Sol$^{\#}$), a significant decrease in the semicircular Nyquist plots is observed on a CN electrode, thus demonstrating that the loose contact between colloids and a fluorine-doped tin oxide (FTO) substrate has been greatly improved

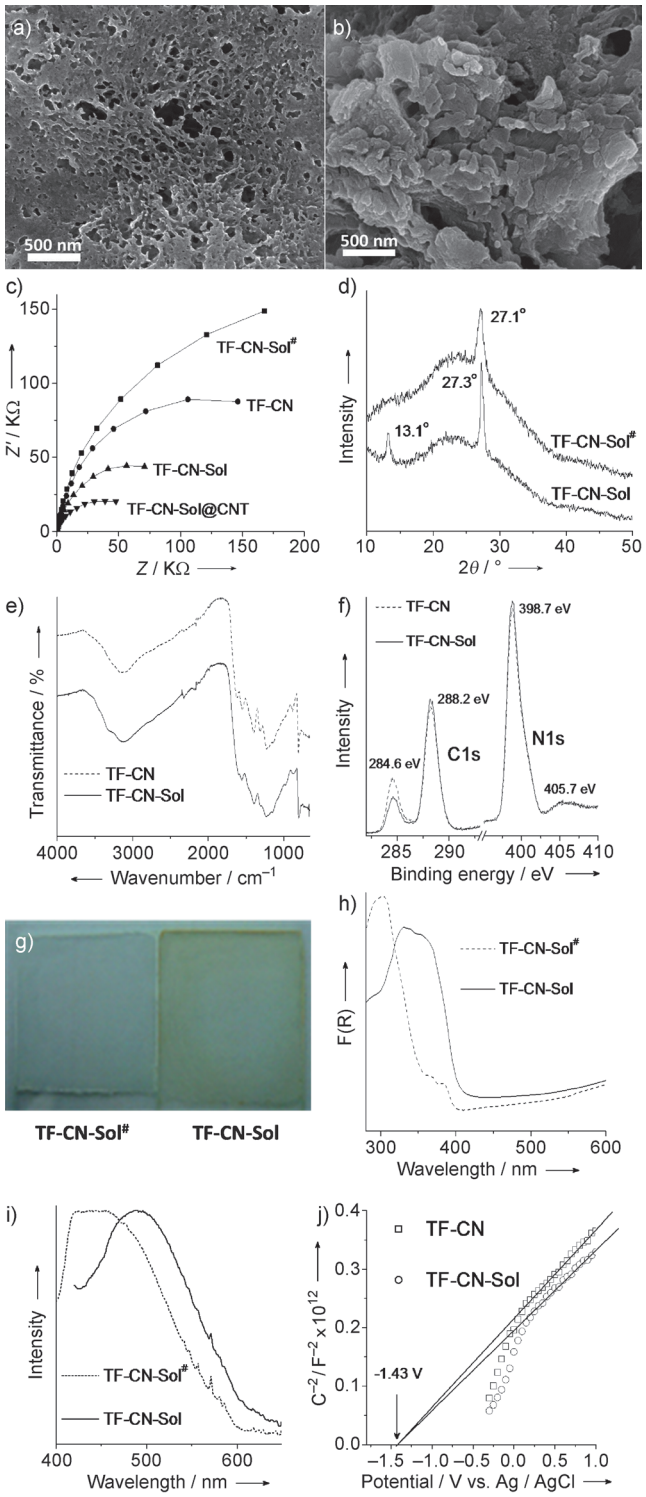

Figure 2. Physical characterization of the CN thin films. a) SEM image of TF-CN-Sol; b) SEM image of TF-CN; c) Nyquist plots measured under −0.2 V versus Ag/AgCl bias potential; d) XRD patterns; e) FTIR spectra; f) XPS spectra; g) photograph of the TF-CN-Sol before (TF-CN-Sol#, left) and after (TF-CN-Sol, right) sintering at 623 K; h) UV/Vis diffuse reflectance spectra; i) PL spectra under excitation at 380 nm; j) Mott–Schottky plots.

by the heat treatment.[7a,b] A Nyquist semicircle with a larger diameter is obtained for a traditional TF-CN electrode, which indicates the poor conductivity for electron transfer. Thus, sol processing with HNO_3 is an efficient pathway for the fabrication of thin-film electrodes with improved electronic conductivity. It should be pointed out that traditional TF-CN without a subsequent heat treatment is unstable in electrolyte solution, and quickly fall offs the substrate, further underlining the advantage of sol processing for film making.

The crystal structure of TF-CN-Sol was characterized by X-ray diffraction (XRD). Two characteristic XRD peaks are always assigned to a typical CN polymer: one is peak (002) at about 27.4° and the other is peak (100) at about 13.1° (see Figure S2 in the Supporting Information).[6a] It is known that the (002) peak originates from the interlayer reflection of a graphite-like structure, while the (100) peak is related to the in-plane structural repeating motifs of the aromatic systems.[6] However, TF-CN-Sol# showed only one peak, namely, peak (002) (Figure 2d), which illustrates that the in-plane periodicity of the aromatic systems has been destroyed through the breakage of the hydrogen bonds by HNO_3 protonation. The slightly low shift of the (002) peak from 27.4° to 27.1° can be attributed to the loose layered structure swollen by H^+ insertion.[11c] As expected, this distorted crystal structure can be easily recovered by subsequent heat treatment at 623 K to completely pyrolyze HNO_3. Thus, both the characteristic (002) and (100) peaks are evident for TF-CN-Sol, and clearly demonstrates that the CN polymer has been perfectly regenerated.

The chemical structure and oxidation state of the C and N backbone elements in TF-CN-Sol were studied by FTIR spectroscopy and X-ray photoelectron spectroscopy (XPS). All of the bands assigned to a typical CN polymer are visible in the FTIR spectrum of TF-CN-Sol (Figure 2e), for example, the skeletal vibrations at 1200–1600 cm^{-1} for aromatic C-N heterocycles and the breathing vibration at 810 cm^{-1} for tri-*s*-triazine subunits.[7] This important finding demonstrates that the core chemical structure of the melon units is robust against HNO_3 etching. No evident change in the binding energies of the C and N backbones of TF-CN-Sol and CN-Sol is evident from XPS characterization, again underlining the excellent chemical inertness of the melon units (Figure 2f). The decrease in the peak intensity at 284.6 eV indicates that the impurities of graphitic carbon species ($C(sp^2)$–$C(sp^2)$ bonds) originating from defective polymerization can be purified by sol processing with HNO_3.[7] This moderate removal of carbon impurities is, in principle, helpful for the optimization of the aromatic π-conjugated system for charge separation, since too many graphitic carbon centers doped in the CN conjugated system will act as defect centers for charge recombination.

The intrinsic semiconductive electronic properties of TF-CN-Sol, such as optical absorption, emission features, and flat-band potential, were carefully examined. After regeneration of the CN structure by heat treatment to completely remove HNO_3, the sample color returns back to yellow (Figure 2g), and the corresponding absorption threshold is 420 nm, but still exhibits a 40 nm blue-shift (Figure 2h). This directly suggests that the aromatic π-conjugated system has been largely recovered, and this band gap enlargement should be attributed to the quantum confinement on reducing the

particle size.[6,7] A similar behavior induced by band gap evolution is observed in the PL spectra, where the emission band of TF-CN-Sol shifts back to a longer wavelength (Figure 2i). The flat-band potential of CN semiconductors can be determined by electrochemical Mott–Schottky plots.[7a] The flat-band potential of TF-CN-Sol was measured to be −1.43 V versus Ag/AgCl, almost the same as the value obtained for typical CN polymers (Figure 2j). Hence, the unique electronic properties of CN can also be largely recovered in the thin film by the heat treatment.

To summarize the above characterizations, a CN polymer with a robust chemical inertness against HNO_3 etching can greatly preserve its unique physicochemical features, in particular the intrinsic semiconductive properties for photoelectrochemical functions.

The high flexibility and compatibility with chemical modifications of the colloidal suspension of CN, as well as its soft nature, also enables broad tunability for the preparation of CN-based nanocomposites with desired functionality for specific applications. A hybrid nanocomposite (CN-Sol@CNTs) made from CN-Sol and carbon nanotubes (CNTs) is shown here as a case study. Experimentally, CNTs previously purified by acid etching are directly dispersed in the CN-Sol solution to give rise to a uniform dark solution (see Figure S3 in the Supporting Information), and the thin-film electrodes (TF-CN-Sol@CNTs) are fabricated by coating the resultant solution on FTO glass for subsequent heat treatment. The CNTs are wrapped well by CN coatings, thereby forming a polymer-based heterostructure (Figure 3a,b). As a consequence of their excellent electrical properties, in particular the high conductivity, the CNTs should function as an efficient pathway for electron transport, fundamentally addressing the poor electronic conductivity of the polymer matrix and allow fast charge separation and collection (Figure 3c). Hence, an evident quenching of the PL intensity (see Figure S3b in the Supporting Information) and a smaller diameter of the Nyquist semicircle (Figure 2c) are realized with TF-CN-Sol@CNTs, thus demonstrating the structural benefits of the hybrid system.[7b]

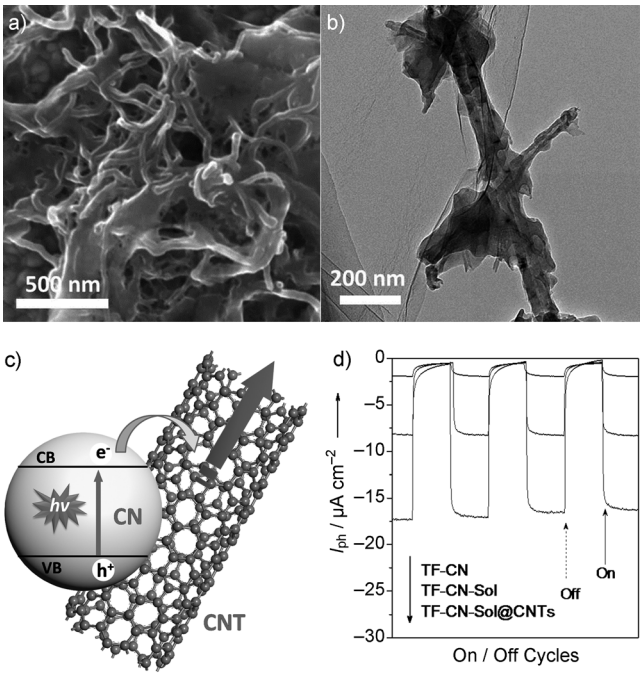

Figure 3. a) SEM and b) TEM images of TF-CN-Sol@CNTs; c) schematic representation of charge transport in the TF-CN-Sol@CNTs hybrid; d) periodic on/off photocurrent response at −0.2 V versus Ag/AgCl bias potential under irradiation with visible light ($\lambda > 420$ nm).

As a consequence of the unique electronic band structure of the CN polymer and the advantages of sol processing for film making, it is of particular interest to use the resultant films as photoelectrodes for solar electricity production. The photocurrent density obtained on a TF-CN-Sol electrode was 8 μA cm^{-2} (Figure 3d), greatly exceeding the value (1.2 μA cm^{-2}) of the traditional TF-CN electrode. This improved efficiency of photocurrent generation should mainly be attributed to the highly interconnected porous networks without significant grain boundaries and the close coating of colloids on the FTO substrate. Moreover, the photoelectrochemical performance can be further enhanced by the integration of CNTs in the polymeric system to promote charge separation, thereby achieving a photocurrent density of 17 μA cm^{-2} with TF-CN-Sol@CNTs. Hence, the sol processing of CN solids with HNO_3 is a promising method for the fabrication of photoactive thin films with improved photoelectrochemistry properties.

Taken together, we have demonstrated that the chemical protonation of CN solids with strong oxidizing acids, for example, HNO_3, is a promising method for the production of a stable colloidal suspension of CN. By taking advantage of the unique features of CN colloids, it is easy to address the problems we always encounter in the fabrication of thin-film electrodes, in particular the abundant boundary defects and the poor contact between particles and substrates. As expected, the thin-film electrodes derived from the CN-Sol demonstrate a remarkably improved performance. Moreover, the high flexibility and compatibility of the colloidal suspension of CN, in principle, enables the polymer system to be modified with desired functionalities, thereby paving the way for the application of CN for specific tasks. For example, hybridizing CN colloids with nanostructural carbons, such as CNTs, activated carbon, and mesoporous carbon membranes, can further advance the unique nitrogen-rich chemistry functions of CN in the oxygen reduction reaction,[13] as a hydrogen evolution catalyst,[14] and as a proton-conductive membrane for gas separation and CO_2 capture.[15]

Keywords: carbon nitride · photo-electrochemistry · polymers · sol-gel processes · thin films

How to cite: *Angew. Chem. Int. Ed.* **2015**, *54*, 6297–6301
Angew. Chem. **2015**, *127*, 6395–6399

[1] a) D. N. Futaba, K. Hata, T. Yamada, T. Hiraoka, Y. Hayamizu, Y. Kakudate, O. Tanaike, H. Hatori, M. Yumura, S. Iijima, *Nat. Mater.* **2006**, *5*, 987; b) C. Liang, Z. Li, S. Dai, *Angew. Chem. Int. Ed.* **2008**, *47*, 3696; *Angew. Chem.* **2008**, *120*, 3754; c) M. S. Mauter, M. Elimelech, *Environ. Sci. Technol.* **2008**, *42*, 5843; d) J. M. Schnorr, T. M. Swager, *Chem. Mater.* **2011**, *23*, 646;

e) C. J. Shearer, A. Cherevan, D. Eder, *Adv. Mater.* **2014**, *26*, 2295; f) F. Béguin, V. Presser, A. Balducci, E. Frackowiak, *Adv. Mater.* **2014**, *26*, 2219.

[2] a) H. W. Kroto, J. R. Heath, S. C. O'Brien, R. F. Curl, R. E. Smalley, *Nature* **1985**, *318*, 162; b) S. Iijima, *Nature* **1991**, *354*, 56; c) K. S. Novoselov, A. K. Geim, S. V. Morozov, D. Jiang, Y. Zhang, S. V. Dubonos, I. V. Grigorieva, A. A. Firsov, *Science* **2004**, *306*, 666; d) M. J. Allen, V. C. Tung, R. B. Kaner, *Chem. Rev.* **2010**, *110*, 132.

[3] a) R. Tenne, *Adv. Mater.* **1995**, *7*, 965; b) L. Zhao et al., *Science* **2011**, *333*, 999; c) J. Du, S. Pei, L. Ma, H.-M. Cheng, *Adv. Mater.* **2014**, *26*, 1958.

[4] a) T.-F. Yeh, J.-M. Syu, C. Cheng, T.-H. Chang, H. Teng, *Adv. Funct. Mater.* **2010**, *20*, 2255; b) L. F. Velasco, J. C. Lima, C. Ania, *Angew. Chem. Int. Ed.* **2014**, *53*, 4146; *Angew. Chem.* **2014**, *126*, 4230; c) K. Gong, F. Du, Z. Xia, M. Durstock, L. Dai, *Science* **2009**, *323*, 760; d) Z.-S. Wu, A. Winter, L. Chen, Y. Sun, A. Turchanin, X. Feng, K. Müllen, *Adv. Mater.* **2012**, *24*, 5130; e) Z.-S. Wu, K. Parvez, A. Winter, H. Vieker, X. Liu, S. Han, A. Turchanin, X. Feng, K. Müllen, *Adv. Mater.* **2014**, *26*, 4552; f) X. Zhuang, F. Zhang, D. Wu, X. Feng, *Adv. Mater.* **2014**, *26*, 3081.

[5] a) H. Rydberg, M. Dion, N. Jacobson, E. Schröder, P. Hyldgaard, S. I. Simak, D. C. Langreth, B. I. Lundqvist, *Phys. Rev. Lett.* **2003**, *91*, 126402; b) M. T. Yin, M. L. Cohen, *Phys. Rev. B* **1984**, *29*, 6996; c) A. Y. Liu, R. M. Wentzcovitch, *Phys. Rev. B* **1994**, *50*, 10362.

[6] a) X. Wang, K. Maeda, A. Thomas, K. Takanabe, G. Xin, J. M. Carlsson, K. Domen, M. Antonietti, *Nat. Mater.* **2009**, *8*, 76; b) Y. Wang, X. Wang, M. Antonietti, *Angew. Chem. Int. Ed.* **2012**, *51*, 68; *Angew. Chem.* **2012**, *124*, 70; c) X. Wang, S. Blechert, M. Antonietti, *ACS Catal.* **2012**, *2*, 1596.

[7] a) J. Zhang, X. Chen, K. Takanabe, K. Maeda, K. Domen, J. D. Epping, X. Fu, M. Antonietti, X. Wang, *Angew. Chem. Int. Ed.* **2010**, *49*, 441; *Angew. Chem.* **2010**, *122*, 451; b) J. Zhang, G. Zhang, X. Chen, S. Lin, L. Möhlmann, G. Dołęga, G. Lipner, M. Antonietti, S. Blechert, X. Wang, *Angew. Chem. Int. Ed.* **2012**, *51*, 3183; *Angew. Chem.* **2012**, *124*, 3237; c) J. Zhang, M. Zhang, R.-Q. Sun, X. Wang, *Angew. Chem. Int. Ed.* **2012**, *51*, 10145; *Angew. Chem.* **2012**, *124*, 10292; d) Y. Zhang, M. Antonietti, *Chem. Asian J.* **2010**, *5*, 1307.

[8] a) T.-Y. Yen, C.-P. Chou, *Solid State Commun.* **1995**, *95*, 281; b) T. Yen, C.-P. Chou, *Appl. Phys. Lett.* **1995**, *67*, 2801; c) Y. Suda, T. Nakazono, K. Ebihara, K. Baba, S. Aoqui, *Carbon* **1998**, *36*, 771; d) M. Y. Chen, P. T. Murray, *J. Vac. Sci. Technol. A* **1998**, *16*, 2093.

[9] M. Shalom, S. Gimenez, F. Schipper, I. Herraiz-Cardona, J. Bisquert, M. Antonietti, *Angew. Chem. Int. Ed.* **2014**, *53*, 3654; *Angew. Chem.* **2014**, *126*, 3728.

[10] a) L. Nahar, I. U. Arachchige, *JSM Nanotechnol. Nanomed.* **2013**, *1*, 1004; b) J. M. Nedelec, *J. Nanomater.* **2007**, *2007*, 36392.

[11] a) B. V. Lotsch, M. Döblinger, J. Sehnert, L. Seyfarth, J. Senker, O. Oeckler, W. Schnick, *Chem. Eur. J.* **2007**, *13*, 4969; b) P. Niu, L. Zhang, G. Liu, H.-M. Cheng, *Adv. Funct. Mater.* **2012**, *22*, 4763; c) T. Y. Ma, Y. Tang, S. Dai, S. Z. Qiao, *Small* **2014**, *10*, 2382.

[12] Y. Zhang, A. Thomas, M. Antonietti, X. Wang, *J. Am. Chem. Soc.* **2009**, *131*, 50.

[13] a) Y. Zheng, Y. Jiao, J. Chen, J. Liu, J. Liang, A. Du, W. Zhang, Z. Zhu, S. C. Smith, M. Jaroniec, et al., *J. Am. Chem. Soc.* **2011**, *133*, 20116; b) J. Liang, Y. Zheng, J. Chen, J. Liu, D. Hulicova-Jurcakova, M. Jaroniec, S. Z. Qiao, *Angew. Chem. Int. Ed.* **2012**, *51*, 3892; *Angew. Chem.* **2012**, *124*, 3958.

[14] J. Duan, S. Chen, M. Jaroniec, S. Z. Qiao, *ACS Nano* **2015**, *9*, 931.

[15] a) Q. Li, J. Yang, D. Feng, Z. Wu, Q. Wu, S. S. Park, C.-S. Ha, D. Zhao, *Nano Res.* **2010**, *3*, 632; b) S.-H. Chai, P. F. Fulvio, P. C. Hillesheim, Z.-A. Qiao, S. M. Mahurin, S. Dai, *J. Membr. Sci.* **2014**, *468*, 73.

Received: February 3, 2015
Revised: March 10, 2015
Published online: April 1, 2015

